Efficient Ray Tracing for Radio Channel Characterization of Urban Scenarios

Daniela Naufel Schettino, Fernando J. S. Moreira, and Cássio G. Rego

Department of Electronics Engineering, Federal University of Minas Gerais, Belo Horizonte, MG 31210-901, Brazil

This paper presents an efficient ray tracing algorithm for the use of the uniform theory of diffraction (UTD) in radio channel characterizations of urban environments. The algorithm is based on a 2-D image theory, which is properly modified to yield 3-D ray trajectories. Multiple reflections and diffractions are considered through the classification of multipath components into four different categories. The adoption of such ray classes eliminates redundant calculations throughout the ray-tracing process, improving the analysis of the electromagnetic propagation over the coverage area.

Index Terms—**Radio channel characterization, radio wave propagation, ray tracing, uniform theory of diffraction (UTD).**

I. Introduction

THE growing demand for mobile communications, specially in urban areas, leads toward the adoption of the microcellular concept. It is then desirable to perform accurate coverage predictions in micro- and pico-cells to minimize on-site measurements. The uniform theory of diffraction (UTD) has been extensively applied in the characterization of radio wave propagation through urban scenarios [1]–[5]. The UTD is an asymptotic technique, based on ray tracing for the definition of the optical paths from the transmitter (T) to a receiver (R).

The first step toward the evaluation of the propagated field based on UTD is the determination of the multipath components (rays) between T and R. Ray-tracing algorithms demand large computational efforts and must be extremely efficient, especially in the analysis of complex urban scenarios. Such algorithms are generally based on shooting-and-bouncing ray (SBR) or imagetheory (IT) techniques [1]. In principle, IT is more rigorous than SBR, as the former can determine all ray-path components—including diffracted rays—without redundancies. The IT uses optical images of the transmitter and diffraction points, considering the obstacle surfaces as reflectors.

Here, we propose a ray-tracing algorithm based on the IT, where only direct, reflected and diffracted components are considered. Ray paths are then formed from combinations among those components, with a maximum number of N_R reflections and N_D diffractions. The UTD is further applied to asymptotically evaluate the electromagnetic field associated with each multipath component.

In order to predict the radio coverage over a certain urban region, observers (receivers) are placed over the area of interest. The ray tracing and the asymptotic evaluation of the scattered field are then determined for each observer. However, the determination of the multipath components that reach each observer can be very time consuming. So, the main objective of the present work is to present a technique where multiple reflections and diffractions are considered via the ray-path classification into four different categories: T-R, T-D, D-D, D-R, where D represents a diffraction point. As only reflections are permitted inside each category, their attainment is a uniform process. The complete ray paths between T and R, accounting for multiple reflections and diffractions, are determined by concatenating elements of the above categories, allowing a single calculation and storage of subtrajectories appearing in different paths.

Initially, a 2-D algorithm traces the trajectories. The adopted 2-D algorithm, which is the core of the present procedure, is based on [3], and incorporates the ray-path classification previously cited. The 2-D rays are then converted into 3-D ones, according to [4]. In the process, reflections from ground and the finite heights of obstacles (e.g., buildings of the urban environment) are appropriately accommodated. A case study will be presented, illustrating the advantages of using the above mentioned ray-path classification.

II. Efficient Ray-Tracing Algorithm

The environment of the urban radio channel will be represented by an approximate model: the obstacles (e.g., buildings) are modeled as cylinders with finite heights and placed perpendicularly over a flat ground, as illustrated in Fig. 1. Initially, a 2-D ray tracing is performed and, during such procedure, the obstacles are momentarily assumed infinitely high and represented by a horizontal cut describing their cross sections, as depicted in Fig. 1. Within this 2-D scenario, the aim is to obtain optical paths from T to R. For that, the concepts defined, for example, in [3] (i.e., image theory, radiation area, segment visibility, *quadtree*, etc.) can efficiently determine the desired 2-D trajectories.

In this section, the techniques used to carry out the 2-D ray tracing are presented. Initially, the techniques adopted in the determination of the multiple reflections, based on IT, are discussed. Then, we consider the inclusion of diffracted rays into the algorithm. Furthermore, we classify the ray subtrajectories into four categories: T-R (e.g., direct ray), T-D, D-D, and D-R. Such classification yields an efficient determination of the complete ray paths from T to R with arbitrary numbers of reflections and diffractions in between. At last, it will be presented the conversion of the 2-D paths into 3-D paths, with some restrictions in the considered trajectories.

Digital Object Identifier 10.1109/TMAG.2006.890976

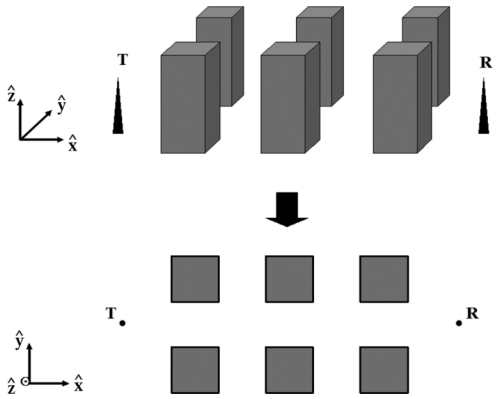

Fig. 1. Two-dimensional description of an urban environment.

Once the trajectories are determined, the reflected and diffracted electric fields are determined by the UTD formulation, described as [6]

$$\mathbf{E}^r(O,\omega) = \overline{\mathbf{R}}(\omega)\mathbf{E}^i(Q_r,\omega)A^r(s)\exp(-jks), \quad (1)$$

$$\mathbf{E}^d(O,\omega) = \overline{\mathbf{D}}(\omega)\mathbf{E}^i(Q_d,\omega)A^d(s)\exp(-jks) \quad (2)$$

where $\mathbf{E}^r$ and $\mathbf{E}^d$ are the reflected and diffracted electric fields at the observation point O, respectively, $\mathbf{E}^i$ is the incident electric field at the reflection (Q_r) or diffraction (Q_d) point, $\overline{\mathbf{R}}$ and $\overline{\mathbf{D}}$ are the UTD reflection and diffraction dyadics, respectively, A^r and A^d are the UTD reflection and diffraction attenuation factors, respectively, and s is the distance measured along the trajectory of the TEM wavefront [6].

A. Reflected Rays

The IT is used to determine the reflected ray paths [3]. The transmitter (T) is successively reflected by the planar faces of the many obstacles, in order to find all the optical paths toward the receiver (R). This is accomplished by locating the transmitter's images with respect to their mirroring surfaces (represented by the cross-section segments in the 2-D model). Then, each one of these images goes through the same process, i.e., the images determined in the preceding iteration are used as (virtual) sources in the present iteration, forming a set of second order images. This process is successively repeated until a predetermined number of image levels is attained, where such number is given by the maximum number of reflections $(\mathrm{N_R})$ to be considered [3].

The successive images of T are organized in a hierarchical fashion tree, where the tree's root is the transmitter (T). The next level of the tree contains the first-order images of T, generated by the many obstacle mirroring faces. The second level contains the second order images (i.e., the images of the first order images), and so on. Throughout the process, several images do not need to be considered and, consequently, stored in the tree. First of all, since not all the faces are reflectors to the (virtual) source, many of them will not contribute to the image's tree and can be immediately discarded. If this is not the case, there are still two possibilities that can preclude the image formation and, if detected *a priori*, applied to save memory space used to store the tree. One is based on the fact that only the faces partially or totally contained within the *lit region* of the (virtual) source can contribute to the formation of the next-level images [3]. Besides, the contribution will occur only if such face is not totally obstructed by another face in the lit region. Such acceleration techniques make the ray-tracing procedure very efficient, mostly for those scenarios where many obstacles are present [3].

After determining all the necessary high-order images of T, the reflection points over the mirroring faces are identified by the image method. This is accomplished by connecting the observation point to an image stored in the tree, forming a segment that must intercept the mirroring face at the corresponding reflection point, which is then properly located and stored. If such intersection does not occur, such path is disregarded and the process continues with the investigation of a different reflected path. The procedure is performed for all the images stored in the tree. The first-level images generate single reflected rays. The second-level images generate double reflected rays, and so forth. Consequently, in order to trace rays with a maximum number of $\mathrm{N_R}$ reflections, images up to the $\mathrm{N_R}$th level must be considered. At the end of the process, the paths that form the T-R category (i.e., rays from T to R with or without reflections in between) are established.

Finally, note that the very same procedure can be extended to those cases where the observer is a diffraction point (D) instead of a receiver (R). So, a similar procedure is applied to obtain the elements of the categories T-D (i.e., rays from T to a given diffraction point D at an obstacle edge, with or without reflections in between).

B. Diffracted Rays

The inclusion of diffraction effects is extremely important, especially in regions where severe blockage mechanisms are present (a common situation in urban environments). In order to determine the diffracted ray-paths, first we need to locate the associated diffraction points (D) over the obstacles' edges. In the 2-D scenario of Fig. 1, such edges are represented by the cross-section vertices. In principle, each diffraction point (i.e., each vertex) is considered a transmitting source. Consequently, image trees are constructed for each one of these vertices, similarly to the procedure described in Section II-A for T (the main difference is that adjacent segments with a common vertex D do not produce first-level images of D). Once the $\mathrm{N_R}$ levels of images of D are determined and stored in the corresponding tree, the subtrajectories that leave D and arrive at R, after many (or none) reflections, are determined and properly classified into the D-R category.

The above trees are also employed to establish the elements of the D-D category. For that, one just needs to replace R by a certain diffraction point D in the algorithm described in the previous paragraph. In this case, it is worthwhile to mention that once the paths between two diffraction points $\mathrm{D_m}$ and D_n are determined, the paths between D_n and $\mathrm{D_m}$ are directly obtained by reversing the orientation of the previous paths. Also, note that $\mathrm{D_m}$ and D_n can represent the same diffraction point (with at least one reflection between them).

C. Ray Categories

The procedure that determines the multipath components between T and R, considering multiple reflections and diffractions, starts by the definition of the elements (i.e., subtrajectories) of the four categories (T-R, T-D, D-D, and D-R), as described in Sections II-A and II-B. Note that such subtrajectories just contain multiple (or none) reflections between the initial and end

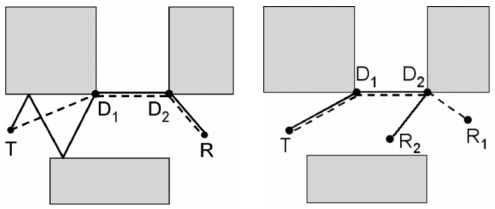

Fig. 2. Different 2-D paths from T to R sharing the same subtrajectories: (a) fixed receiver and (b) different receivers.

points. After that, the ray paths between T and R are determined by properly concatenating subtrajectories from each category, with a maximum of N_R reflections and ND diffractions permitted for each path.

For instance, the paths between T and R that do not suffer any diffraction are directly obtained from the trajectories stored in the T-R category. To determine ray paths passing through a single diffraction point (D_m), it is necessary to pick up T-D subtrajectories that leave T and arrive at D_m and concatenate them with D-R subtrajectories that leave D_m and arrive at R, just allowing a maximum of N_R reflections. If rays with several diffractions are to be considered, one just need to include D-D subtrajectories between the elements of T-D and D-R categories. For example, a ray from T to R with two diffractions (at D_1 and D_2, respectively) is build from the concatenation of three subtrajectories with the sequence T–D_1, D_1–D_2, and D_2–R, as illustrated in Figs. 2(a) and (b).

In Fig. 2(a), one observes two different ray paths between T and R, but sharing two subtrajectories (one D-D and the other D-R). In Fig. 2(b), a common situation is depicted: the need for several receivers in order to characterize a certain coverage area. From the figure, one observes that ray paths arriving at different points may share subtrajectories (a T-D and a D-D in this case). Figs 2(a) and (b) illustrates the most important feature in adopting the categories T-R, T-D, D-D, and D-R in the ray-tracing algorithm: the avoidance of redundant calculations of subtrajectories that appear in several paths between T and R. The proposed algorithm also has an extra feature: for each different location of R, only subtrajectories T-R and D-R must be recalculated, as far as T is kept in the same position [see Fig. 2(b)]. So, the algorithm is suited to characterize large outdoor urban environments with multiple receivers.

To complete the ray tracing process, it is necessary to convert the 2-D paths into 3-D ones, which is discussed next.

D. Conversion of 2-D Rays Into 3-D Rays

The 2-D rays are converted into their 3-D counterparts following the procedure detailed in [4]. The ground is assumed flat, such that all vertical obstacle edges are perpendicular to ground and, consequently, parallel to each other. Ground reflections are accounted for by simply applying the image method to T (or R) with respect to ground [4], as illustrated in Fig. 3. Consequently, each 2-D path between T and R generates two 3-D trajectories: one that reflects once at ground reaching R and another that does not, independently of the number of reflections and diffractions at obstacles (see Fig. 3). Actually, the 2-D path is the projection of the 3-D counterparts over the ground plane, as one can inspect from Fig. 3. The conversion of 2-D ray path into 3-D

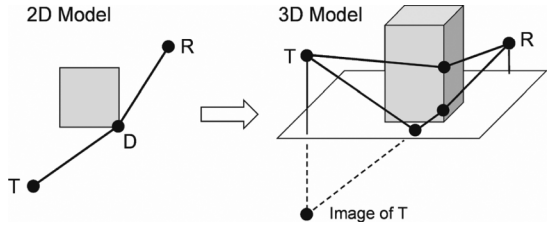

Fig. 3. The 3-D counterparts of the 2-D ray path.

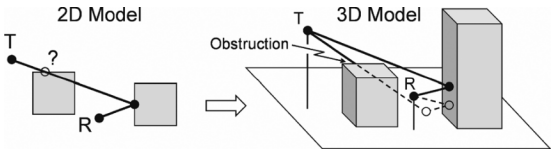

Fig. 4. The 3-D obstruction considerations.

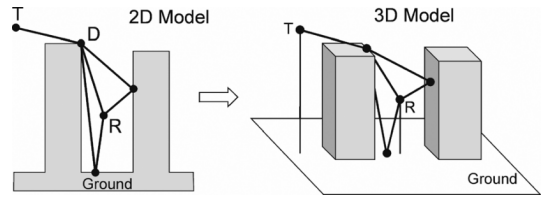

Fig. 5. The 2-D extension in the plane of incidence to account for top-edge diffractions.

trajectories is performed with the help of the total distance measured along the 2-D path and the antennas heights with respect to the ground [4].

For the 3-D path to be considered a true ray, it cannot be obstructed by any obstacle. So, after obtaining the 3-D trajectories, one must apply an algorithm to test for possible obstructions and, consequently, eliminate the obstructed paths. Obstruction tests must take into account the trajectories' and obstacles' heights, assuring that several rays that would be discarded in a pure 2-D algorithm are considered if passing above an obstacle, as shown in Fig. 4.

In the present model, reflections and diffractions on the obstacles' tops cannot be generally considered, except at the plane of incidence defined by T and R. Rays at this plane, diffracted or reflected at the obstacles' tops, are easily included by simply extending the proposed 2-D algorithm from the horizontal plane (parallel to ground) to the plane of incidence, as illustrated in Fig. 5 for a top diffraction. Here, ground reflections are automatically included and, consequently, each 2-D path generates just a single 3-D path.

III. Case Study

The determination of the multipaths with the help of the four subtrajectory categories T-R, T-D, D-D, and D-R avoid redundant calculations and memory storage, as explained in Section II. Consequently, great savings on computer effort are attained, for many of the subtrajectories appear several times in different paths.

In order to demonstrate the usefulness of the ray tracing techniques presented in Section II, a practical case study is investigated. It consists of 17 obstacles (i.e., 17 buildings), comprising 80 faces and edges, as illustrated in Fig. 6. The scenario represents the core of Ottawa, Canada, for which UTD-based results [5] and measurements [7] for the vertical polarization at 910 MHz

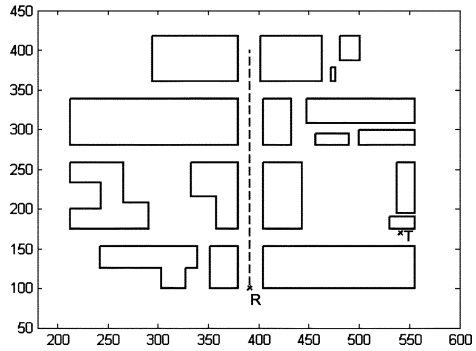

Fig. 6. Plane view of the Ottawa city core. The transmitter is at T and receivers (R) are placed along Bank St. (dotted line).

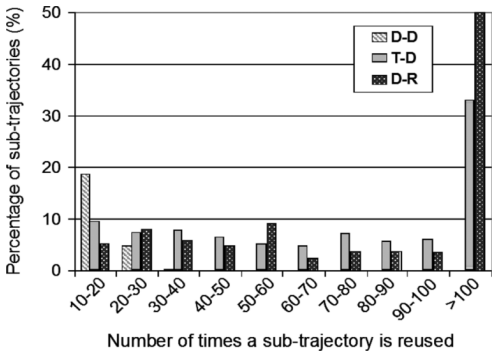

Fig. 7. Distribution of T-D, D-D, and D-R subtrajectory reuse for a receiver at (391 m, 100 m), as indicated in Fig. 6.

are available in the literature. Fig. 6 also depicts the transmitter (T) and receivers (dotted line) locations, with heights equal to 8.5 m and 3.65 m, respectively. More details about the geometrical and electrical features can be obtained in [5] and [7].

The ray-tracing algorithm of Section II was applied, considering 3-D trajectories from T to R with five reflections and two diffractions, at most. To illustrate the subtrajectory redundancies avoided by the present algorithm, Fig. 7 shows the distribution of reused subtrajectories T-D, D-D, and D-R for a single receiver located at (391 m, 100 m), as pointed out in Fig. 6. The results indicate that some subtrajectories, particularly T-D and D-R ones, are reused more than a hundred times even for a single R. When several receivers are considered (for a proper radio-channel characterization), the amount of subtrajectory reuse increases tremendously. The results depicted in Fig. 7 illustrate the improvement attained by the present ray-tracing algorithm when compared with other algorithms that do not take advantage of storing subtrajectories instead of complete trajectories between T and R [3], [4].

For the urban environment of Fig. 6, 150 receivers where placed along the dotted line (Bank St.), with intervals of 2 m. As T was kept fixed, the elements of the T-D and D-D categories were calculated just once, improving the processing time of the ray-tracing routine. Consequently, only the T-R and D-R elements needed to be recalculated for each different receiver. For the scenario depicted in Fig. 6, the reuse of the T-D and D-D elements alone was responsible for a 60% reduction in the processing time. Finally, Fig. 8 illustrates path loss predictions along Bank St. (marked with a dotted line in Fig. 6). The UTD estimates were obtained with the help of the ray-tracing algorithm presented in Section II. The measured data was obtained

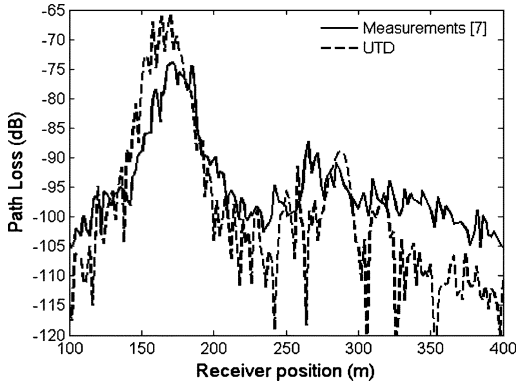

Fig. 8. UTD-predicted and measured path loss for the urban environment depicted in Fig. 6 for a vertical polarization at 910 MHz.

from [7]. From the results one can observe the usefulness of the UTD for coverage predictions in urban scenarios.

IV. Conclusion

This paper presented an efficient ray-tracing algorithm for the UTD characterization of radio wave propagation in urban environments. The ray paths are decomposed into subtrajectories, which are classified in four categories: T-R, T-D, D-D, and D-R. The ray trajectories between T and R are established by appropriately concatenating the several category elements. Such procedure avoids redundant calculations of subtrajectories and allows the reuse of the same T-D and D-D subtrajectories for different receiver locations. The technique was demonstrated in a real-life radio-channel characterization, where the concatenation procedure reduced the processing time by more than a half. Path loss estimates provided by a UTD analysis were compared against measurements to demonstrate the applicability of the proposed technique.

Acknowledgment

This work was supported in part by CNPq and CAPES, Brazil.

References

[1] Z. Ji, B.-H. Li, H.-X. Wang, H.-Y. Chen, and T. Sarkar, "Efficient ray-tracing methods for propagation prediction for indoor wireless communications," *IEEE Antennas Propagat. Mag.*, vol. 43, no. 2, pp. 41–49, Apr. 2001.

[2] J. Richter, M. O. Al-Nuaimi, and L. P. Ivrissimtzis, "Optimization of radio coverage in urban microcells using a UTD based ray-tracing model," *Proc. Inst. Electron. Eng.–Microw. Antennas Propagat.*, vol. 151, no. 3, pp. 187–192, Jun. 2004.

[3] F. A. Agelet, F. P. Fontan, and A. Formella, "Fast ray-tracing for microcellular and indoor environments," *IEEE Trans. Magn.*, vol. 33, no. 2, pp. 1484–1487, Mar. 1997.

[4] H.-W. Son and N.-H. Myung, "A deterministic ray tube method for microcellular wave propagation prediction model," *IEEE Trans. Antennas Propagat.*, vol. 47, no. 8, pp. 1344–1350, Aug. 1999.

[5] S. Y. Tan and H. S. Tan, "Propagation model for microcellular communications applied to path loss measurements in Ottawa City streets," *IEEE Trans. Veh. Technol.*, vol. 44, no. 2, pp. 313–317, May 1995.

[6] R. G. Kouyoumjian and P. H. Pathak, "A uniform geometrical theory of diffraction for an edge in a perfectly conducting surface," *Proc. IEEE*, vol. 62, no. 11, pp. 1448–1461, Nov. 1974.

[7] J. H. Whitteker, "Measurements of path loss at 910 MHz for proposed microcell urban mobile systems," *IEEE Trans. Veh. Technol.*, vol. 37, no. 3, pp. 125–129, Aug. 1988

Manuscript received April 24, 2006 (e-mail: schett@cpdee.ufmg.br).